Improved cell-penetrating peptide–PNA conjugates for splicing redirection in HeLa cells and exon skipping in *mdx* mouse muscle

Gabriela D. Ivanova[1], Andrey Arzumanov[1], Rachida Abes[2], Haifang Yin[3], Matthew J. A. Wood[3], Bernard Lebleu[2] and Michael J. Gait[1,*]

[1]Medical Research Council, Laboratory of Molecular Biology, Hills Road, Cambridge CB2 0QH UK, [2]UMR 5235 CNRS, Université Montpellier 2, Place Eugene Bataillon, 34095 Montpellier cedex 5, France and [3]Department of Physiology, Anatomy and Genetics, University of Oxford, Oxford OX1 3QX, UK

ABSTRACT

Steric blocking peptide nucleic acid (PNA) oligonucleotides have been used increasingly for redirecting RNA splicing particularly in therapeutic applications such as Duchenne muscular dystrophy (DMD). Covalent attachment of a cell-penetrating peptide helps to improve cell delivery of PNA. We have used a HeLa pLuc705 cell splicing redirection assay to develop a series of PNA internalization peptides (Pip) conjugated to an 18-mer PNA705 model oligonucleotide with higher activity compared to a PNA705 conjugate with a leading cell-penetrating peptide being developed for therapeutic use, (R-Ahx-R)$_4$. We show that Pip–PNA705 conjugates are internalized in HeLa cells by an energy-dependent mechanism and that the predominant pathway of cell uptake of biologically active conjugate seems to be via clathrin-dependent endocytosis. In a mouse model of DMD, serum-stabilized Pip2a or Pip2b peptides conjugated to a 20-mer PNA (PNADMD) targeting the exon 23 mutation in the dystrophin gene showed strong exon-skipping activity in differentiated *mdx* mouse myotubes in culture in the absence of an added transfection agent at concentrations where naked PNADMD was inactive. Injection of Pip2a-PNADMD or Pip2b-PNADMD into the tibealis anterior muscles of *mdx* mice resulted in ~3-fold higher numbers of dystrophin-positive fibres compared to naked PNADMD or (R-Ahx-R)$_4$-PNADMD.

INTRODUCTION

Sequence-specific steric blocking oligonucleotides (ON) that target intra-cellular RNAs have excellent potential for development as therapeutic agents for a variety of diseases (1,2). In contrast to standard antisense or siRNA, there is no requirement for recognition of the ON–RNA hybrid by a cellular enzyme complex (such as RNase H or RISC) in order to achieve biological activity. Instead, the ON is targeted at a specific RNA site to inhibit or alter an essential function or protein recognition merely by ON–RNA hybrid formation and resultant steric interference. This approach may have higher specificity than those dependent on RNA cleavage since binding at an incorrect site is less likely to trigger a biological effect. Further it allows a greater variety of ON chemistry to be explored and hence a better opportunity to adjust both cell delivery and pharmacology.

The steric block approach is particularly useful to interfere with specific pre-mRNA processing in the cell nucleus and hence to alter gene expression. For example, a number of clinically relevant applications involve the redirection of splicing, where ONs are targeted at a splice site or at splicing regulating sequences (3). The most clinically advanced disease target of this type is Duchenne muscular dystrophy (DMD). DMD is an X-linked muscle disorder caused mainly by nonsense or frame-shift mutations in the dystrophin gene, occurring with a frequency of about one in 3500 live male births. DMD patients suffer from severe, progressive muscle wasting, whereas the milder Becker muscular dystrophy (BMD) is caused by in-frame deletions resulting in expression of a shortened but partially functional protein. ONs have been shown to induce targeted 'exon skipping' to correct the reading frame of mutated dystrophin mRNA such that shorter dystrophin forms are produced with activity similar to that of BMD (4).

Many types of ON have been investigated in a mouse muscle cell model and also in an *mdx* dystrophic mouse model, where a nonsense mutation in exon 23 is skipped to restore dystrophin production (5–8). Initially 2′-*O*-methyl phosphorothioate (2′OMePS) ONs were used to target the human dystrophin gene (9,10). This backbone has been

taken to a Phase I clinical trial in Holland targeting exon 51 of dystrophin pre-mRNA in DMD patients involving intramuscular injection with promising results in localized dystrophin production (11). A similar Phase I trial is currently in progress in the UK involving use of a 30-mer phosphorodiamidate morpholino oligonucleotide (PMO) (12). Studies *in vivo* have suggested higher levels of exon skipping and restoration of dystrophin expression using PMO compared to 2′OMePS (8,12). PMOs are non-ionic ONs and are less likely to form unwanted interactions with other intra-cellular molecules of target cells. PMOs have been used in animal models of disease and several clinical trials to date (13). Very recently Yin *et al.* (14) have demonstrated that use of a second non-ionic ON type, known as peptide nucleic acid (PNA), also leads to a significant increase in the number of dystrophin-positive fibres when PNA targeted to the exon 23 mutation was injected into the tibialis anterior (TA) muscles of *mdx* mice, and with a higher efficiency than a naked 2′OMePS ON.

However, a key issue in use of ONs as therapeutics has been to achieve a sufficient level of intra-cellular delivery, especially *in vivo* for example within diseased muscle of DMD patients, such that the ON is in significant excess over the RNA target and remains so in order to achieve a high and sustained level of biological activity. Conjugation of the ON to a cell-penetrating peptide (CPP) enhances significantly the activity of both PNA and PMO in cellular and animal models (15–19). In the case of PMO, an arginine-rich lead peptide has been proposed, (R-Ahx-R)$_4$-Ahx-β-Ala (or RXR4XB), where Ahx (X) is aminohexanoyl. This peptide takes into account the key roles played by Arg side chains in CPP uptake. Several examples of enhanced activity of RXR4XB-PMO over naked PMO have been published in both cell and animal models (2,13), including recently in DMD studies through intraperitoneal injection into *mdx* mice (20).

To assess the intra-nuclear activity levels of CPP-ON conjugates, we have used a well-established HeLa cell assay that involves splicing redirection of an aberrant β-globin intron by an 18-mer synthetic ON (targeted to the 705 site) and subsequent upregulation of firefly luciferase (21). This assay is straightforward and has a high dynamic range, allowing both high- and low-activity levels to be measured quantitatively as a positive luminescence read-out. In addition the EC_{50} of the splicing redirection can be assessed readily at the RNA level by an RT-PCR assay. We showed that an RXR4XB–PMO705 conjugate had significant splicing redirection activity in the luciferase upregulation model at 1 μM concentration (22). Similarly we showed that a RXR4–PNA705 conjugate also had significantly better splicing redirection activity (23) than could be achieved with other well-known CPPs, such as Tat, Penetratin, R$_9$ or K$_8$ (24–26). We (23,26–29) and other groups (30,31) have shown that the major barrier for nuclear delivery of CPP–PNA, required for splicing redirection, is release from endocytotic vesicular compartments. Indeed, polycationic CPPs are internalized by an active mechanism of endocytosis, which involves electrostatic interactions with cellular heparan sulphates, and have little access to

the nuclear compartment (27). Thus, for many standard CPPs conjugated to PNA, endosomolytic agents, such as chloroquine, calcium ions or high sucrose concentration (28,32), are necessary to obtain a significant splicing redirection activity (23–26). Therefore, the key to improving activity levels further is to search for CPPs that can trigger enhanced endosomal release.

We described recently R$_6$-Penetratin (R6Pen), a derivative of Penetratin in which six Arg residues were added to the N-terminus of the CPP. Activity was observed in an HIV-1 *trans*-activation inhibition assay that requires nuclear delivery when R6Pen was disulphide-conjugated to a PNA complementary to the *trans*-activation responsive element RNA (28). We also showed that R6Pen disulphide or stably conjugated to PNA705 gave significantly better upregulation of luciferase in the splicing redirection assay than a number of other CPP–PNA705 conjugates, including RXR4-PNA705, at both protein and RNA levels and showed an EC_{50} of ~1 μM (33).

Starting with the R6Pen lead, we have now designed a series of PNA internalization peptides (Pip) with retained or improved activity in the HeLa cell splicing redirection assay when conjugated to PNA705 and which are better stabilized to serum proteolysis. We show that Pip–PNA705 conjugates are internalized in HeLa cells by an energy-dependent mechanism and predominantly via clathrin-dependent endocytosis. Conjugates of Pip2a or Pip2b to a 20-mer PNA targeted to the exon 23 *mdx* mutation (PNADMD) showed strong exon-skipping activity in differentiated *mdx* mouse myotubes and a higher number of dystrophin-positive fibres when injected into the TA muscles of *mdx* mice compared to naked PNADMD or RXR4-PNADMD.

MATERIALS AND METHODS

Synthesis of peptide–PNA conjugates

Synthesis of PNA. N-terminal nitropyridyl (Npys) cysteine-containing PNA705 (NH$_2$-Cys(NPys)-Lys-CCT CTTACCTCAGTTACA-Lys-amide) was synthesized on an Apex 396 Synthesizer (Advanced ChemTech) or on a Liberty microwave peptide synthesizer (CEM) by the Fmoc/Bhoc method as previously described (28,34). Batches of naked 20-mer PNADMD (GGCCAAAC CTCGGCTTACCT), sense 20-mer PNA control sequence AGGTAAGCCGAGGTTTGGCC and PNADMD for thioether conjugation (N-α-bromoacetyl-NH-Lys-GGCC AAACCTCGGCTTACCT-Lys-amide) were obtained from Panagene (Korea) or synthesized in house on a Liberty microwave peptide synthesizer. N-terminal bromoacetylation was carried out by the method previously reported (35).

MALDI-TOF mass spectrometry was carried out on a Voyager DE Pro BioSpectrometry workstation with a matrix of α-cyano-4-hydroxycinnamic acid, 10 mg ml^{-1} in acetonitrile/3% aqueous trifluoroacetic acid (1:1, v/v). The accuracy of the mass measurement in linear mode is regarded by the manufacturer as ±0.05%, but since internal calibration was not used, the determined values varied in a few cases from the calculated by ±0.1%.

Synthesis of peptides. All peptides were prepared with free N-terminus and C-terminal amide and also contained an additional C-terminal cysteine residue to allow conjugation to the PNA. Peptides were synthesized on a PerSeptive Biosystems Pioneer peptide synthesizer (100 μmol scale) using standard Fmoc/*tert*-butyl solid phase synthesis techniques as C-terminal amide peptides using NovaSyn TGR resin (Novabiochem). Deprotection of all peptides and cleavage from the solid support was achieved by treatment with trifluoroacetic acid (TFA) in the presence of triethylsilane (1%), ethane dithiol (2.5%) and water (2.5%). Purification was carried out by reversed phase HPLC as previously described (36) and analysed by MALDI-TOF mass spectrometry with the same matrix as for PNA.

Disulphide conjugations. These were carried out essentially as previously described, usually with a 2.5-fold excess of peptide component over NPys PNA component. Purification was carried out by reversed phase-HPLC as above and analysis by MALDI-TOF mass spectrometry (28,34).

Thioether conjugations. In a typical conjugation reaction, 50 nmol bromoacetyl PNA was dissolved in 50 μl formamide and 25 μl BisTris.HBr buffer (pH 7.5) and 12.5 μl C-terminal-Cys-containing peptide (10 mM, 125 nmol, 2.5 eq.) was added. The solution was heated at 45°C for 2.5 h. The resulting conjugate was purified in one injection by reversed phase-HPLC using a Phenomenex Jupiter C18 (250×10 mm; 10 micron) column, hydrochloric acid-containing buffers (buffer A: 5 mM HCl; buffer B: 5 mM HCl in acetonitrile/water 90/10), a flow rate of 3.5 ml min^{-1} and a gradient of 5–20% buffer B in 25 min when conjugating to Pip peptides, or a gradient of 2 to 15% buffer B in 25 min when conjugating to RXR4 peptide. The product was analysed by MALDI-TOF mass spectrometry.

Splicing redirection assay in HeLa cells

This was carried out similarly to that described previously (23,26). PNA or peptide–PNA conjugates were incubated for 4 h in 1 ml OptiMEM medium with exponentially growing HeLa pLuc705 cells (1.75×10^5 cells/well seeded and cultivated overnight in 24-well plates). The conjugates were diluted with 0.5 ml complete medium (DMEM plus 10% fetal bovine serum) and incubation continued for 20 h. Cells were washed twice with ice-cold PBS and lysed with Reporter Lysis Buffer (Promega, Madison, WI). Luciferase activity was quantified with a Berthold Centro LB 960 luminometer (Berthold Technologies, Bad Wildbad, Germany) using the Luciferase Assay System substrate (Promega, Madison, WI). Cellular protein concentrations were measured with the BCA^{TM} Protein Assay Kit (Pierce, Rockford, IL) and read using an ELISA plate reader (Dynatech MR 5000, Dynatech Labs, Chantilly, VA) at 550 nm. Levels of luciferase expression are shown as relative luminescence units (RLU) per microgram protein or as fold increase in luminescence over background. All experiments were performed in triplicate. Each data point was averaged over the three replicates.

RT-PCR analysis of splicing redirection

For dose-dependence experiment, cells were treated as described above with increasing concentrations of conjugates. After carrying out the luciferase assay and BCA^{TM} Protein Assay, the remaining cell lysates (about 270 μl) were transferred into 2-ml microfuge tubes and total RNA was extracted with 1 ml TRI Reagent (Sigma). Minor changes to the manufacturer's protocol were made to accommodate the presence of Reporter Lysis Buffer. Thus, 0.3 ml of chloroform was used for extraction and the amount of iso-propanol for RNA precipitation was increased to give a 1:1 mixture with the aqueous phase. The extracted RNA was examined by RT-PCR (Genius Techne Thermal cycler) with forward primer 5′-TTG ATA TGT GGA TTT CGA GTC GTC-3′ and reverse primer 5′-TGT CAA TCA GAG TGC TTT TGG CG-3′. The products were analysed on a 2% agarose gel, which was scanned using Gene Tools Analysis Software (SynGene, Cambridge, UK).

Mechanism assays

For studies of energy-dependence, HeLa pLuc705 cells were grown as usual and pre-incubated for 30 min in OptiMEM at 37°C or 4°C. CPP–PNA conjugates were then added at a final concentration of 1 μM and incubation was continued for 1 h. Luciferase expression was monitored as described in the splicing redirection assay section.

For studies of the endocytotic pathway, HeLa pLuc705 cells were grown as usual and pre-incubated for 30 min in OptiMEM at 37°C in the presence of the appropriate inhibitors. CPP–PNA conjugates were then added at a final concentration of 1 μM and incubation was continued for 30 min. Luciferase expression was monitored as described in the splicing redirection assay section. Chlorpromazine (30 μM) or K$^+$ depletion were used to inhibit clathrin-coated pits-mediated endocytosis; nystatin (50 μM) or fillipin-III (5 μg ml^{-1}) were used to inhibit caveolae-mediated endocytosis; methyl-β-cyclodextrin (mBCD) (2.5 mM) or 5-(*N*-ethyl-*N*-isopropyl)-amiloride (EIPA) (1 mM) were used to inhibit macropinocytosis. Endocytosis inhibitors were used at concentrations that did not affect significantly cell metabolism, as judged by the absence of effect on protein synthesis levels (data not shown).

Serum stability assay

CPP–PNA conjugates (20 μM) were incubated in PBS containing 20% mouse serum (prepared by 3×30 min 13 000 r.p.m. centrifugation at 4°C of fresh clotted blood from female Balb/c mice) at 37°C. Aliquots of 10 μl were taken at 0, 15, 30, 60 and 120 min and diluted with 50 μl 10% dichloroacetic acid (DCA) in H$_2$O/CH$_3$CN (50/50). The samples were mixed and kept at –20°C. The precipitated serum proteins were separated by centrifugation (13 000 r.p.m., 5 min) and the supernatant was analysed by MALDI-TOF mass spectrometry.

Exon skipping in mouse *mdx* muscle cells

H2K *mdx* myoblasts were cultured at 33°C under a 10% CO_2 atmosphere in DMEM supplemented with 20% FBS, 1.5% chicken embryo extract (PAA Laboratories Ltd, Yeovil, UK), and 20 U ml^{-1} Interferon γ (Invitrogen). Myotubes were obtained from confluent H2K *mdx* cells seeded in gelatin-coated 12-well plates after 3 days of serum deprivation at 37°C under a 5% CO_2 atmosphere (DMEM with 5% horse serum). The CPP–PNA conjugates were incubated with myotubes for 4 h in 1 ml OptiMEM and then replaced by 2 ml of DMEM/5% horse-serum media for further incubation. After 20 h myotubes were washed twice with PBS and total RNA was extracted with 1 ml of TRI Reagent. RNA preparations were treated with RNase free DNase (2 U) and Proteinase K (20 µg) prior to RT-PCR analysis. The RT-PCR was carried out in 25 µl with 1 µg RNA template using SuperScript III One-Step RT-PCR System with Platinum *Taq* DNA polymerase (Invitrogen) primed by forward primer 5′-CAG AAT TCT GCC AAT TGC TGAG-3′ and reverse primer 5′-TTC TTC AGC TTG TGT CAT CC-3′. The initial cDNA synthesis was performed at 55°C for 30 min followed by 30 cycles of 95°C for 30 s, 55°C for 1 min and 68°C for 80 s. RT PCR product (1 µl) was then used as the template for secondary PCR performed in 25 µl with 0.5 U Super TAQ polymerase (HT Biotechnologies) and primed by forward primer 5′-CCC AGT CTA CCA CCC TAT CAG AGC-3′ and reverse primer 5′-CCT GCC TTT AAG GCT TCC TT-3′. The cycling conditions were 95°C for 1 min, 57°C for 1 min and 72°C for 80 s for 25 cycles. Products were examined by 2% agarose gel electrophoresis.

For the electroporation assays, non-differentiated myoblast cells were seeded 2 days before the electroporation and maintained in 20% FBS/DMEM with Interferon γ at 33°C in 10% CO_2. Cells were treated with trypsin, counted and centrifuged at 1000 r.p.m. for 5 min, then re-suspended in 0.5 ml of Nucleofactor Solution V (Amaxa, Gaithersburg, MD, USA) to give 1.5×10^6 cells/100 µl. 100 µl of cell suspension was mixed with 0.5 nmol of PNA or PNA–peptide conjugate and placed into an Amaxa cuvette. After an electric pulse (program T-020) the cell suspension was mixed with 0.5 ml OptiMEM and incubated in a microfuge tube for 10 min at room temperature. Cells were then transferred into a gelatin-precoated 6-well plate containing 4 ml of 20% FBS/DMEM/Interferon γ and incubated for 24 h at 33°C in 10% CO_2. After two washes with PBS total RNA was extracted with 1.5 ml of TRI Reagent and the PCR carried out as above.

For the cell viability assay (data not shown), myotubes in gelatin-coated 24-well plates were incubated with CPP–PNA conjugates for 4 h in 0.5 ml OptiMEM followed by a further 20-h incubation in 1 ml of DMEM/5% horse serum. Colorimetric MTS cell viability assay was performed using 200 µl/well of CellTiter 96 Aqueous One solution Cell Proliferation Assay (Promega). Each data point was averaged over duplicates of three experiments.

Animals and intramuscular injection

Six- to eight-week-old *mdx* mice were used in all experiments (three mice each in the test and five in control groups). The tibilias anterior (TA) muscle of each experimental *mdx* mouse was injected with 5 µg of PNA or PNA–peptide conjugate in 40 µl of saline at a final concentration of 125 µg ml^{-1}, and the contralateral muscle was injected with saline. The experiments were carried out in the Animal Unit, Department of Physiology, Anatomy and Genetics, University of Oxford, Oxford, UK, according to procedures authorized by the UK Home Office. Mice were killed by cervical dislocation 2 weeks after injection, and muscles were snap-frozen in liquid nitrogen-cooled isopentane and stored at –80°C.

Immunohistochemistry. Sections of 8 µm were cut from at least two-thirds of the muscle length of TA at 100 µm intervals. The sections were then examined for dystrophin expression with a polyclonal antibody 2166 against the dystrophin carboxyl-terminal region (the antibody was kindly provided by Professor Kay Davies). The intervening muscle sections were collected either for RT-PCR analysis and western blot or as serial sections for immunohistochemistry. Polyclonal antibodies were detected by goat-anti-rabbit IgGs. Alexa Fluro 594 (Molecular Probe, UK) and nuclei were counter-stained with DAPI. Dystrophin-positive fibres were counted by fluorescence microscopy using Alexa vision LE software and presented per nanomole compound.

RNA extraction and nested RT-PCR analysis. Total RNA was extracted from TA muscle tissue with Trizol (Invitrogen, UK) and 800 ng of RNA template was used for 20 µl RT-PCR with the OneStep RT-PCR kit (Qiagen, UK). The primer sequences for the initial RT-PCR were as shown above for muscle cell studies and were used for amplification of messenger RNA from exons 20 to 26. The cycle conditions were 95°C for 30 s, 55°C for 1 min and 72°C for 2 min for 25 cycles. RT-PCR product (1 µl) was then used as the template for secondary PCR performed in 25 µl with 0.5 U *Taq* DNA polymerase (Invitrogen, UK). The primer sequences for the second round were the same as shown above for muscle cell studies. The cycle conditions were 95°C for 1 min, 57°C for 1 min and 72°C for 2 min for 25 cycles. The products were examined by electrophoresis on a 2% agarose gel.

RESULTS

We chose to use the HeLa cell splicing redirection assay (33) to monitor the activity levels of derivatives of R6Pen–PNA705 altered in the peptide part. It is convenient to consider the 25-mer R_6Penetratin (R6Pen) peptide as comprising three segments (Figure 1a), an N-terminal oligo-Arg region (segment 1), a central more hydrophobic region (segment 2) and a C-terminal more basic region (segment 3). R6Pen is linked to the PNA via a short Gly–Gly spacer that is conjugated to the PNA via a reducible disulphide or stable thioether linkage to the terminal Cys residue. The resultant conjugate has an EC_{50} of about
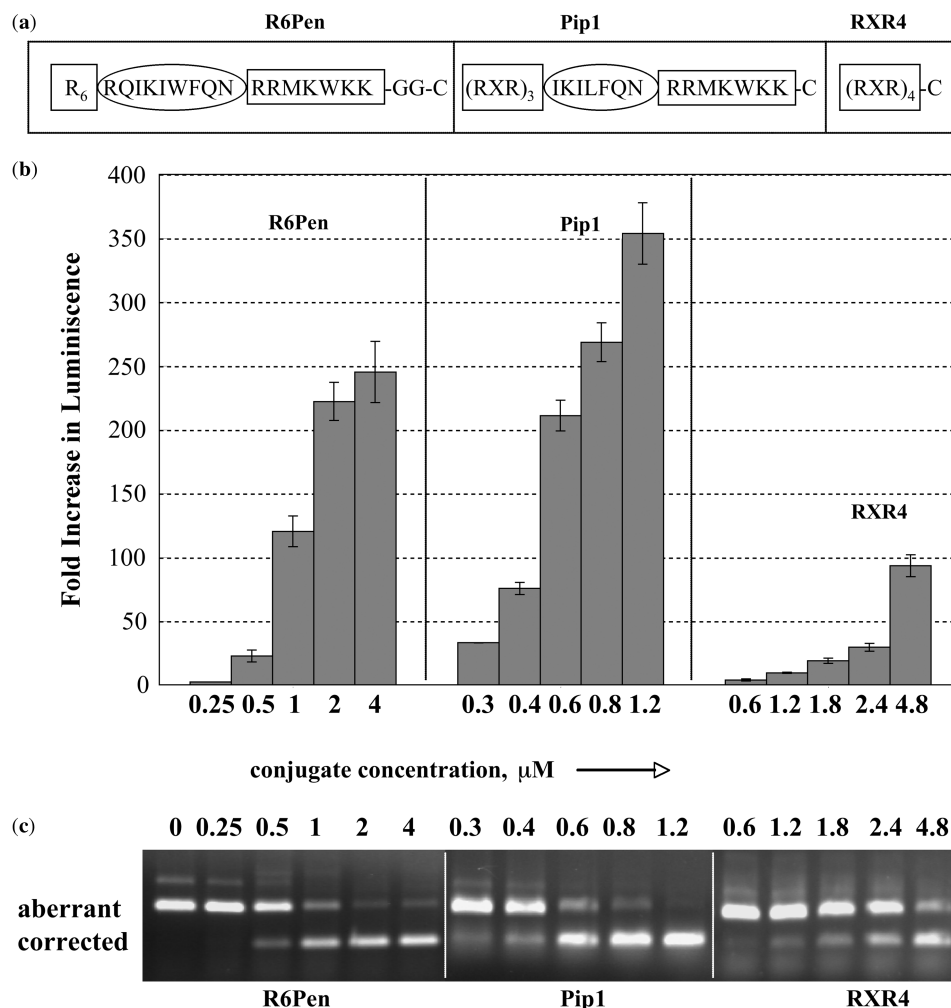
Figure 1. (a) Structures of R6Pen, Pip1 and RXR4 peptides (which are disulphide linked to 18-mer PNA705) showing the three segments ringed or boxed; (b) splicing redirection activity as measured by fold luminescence increase for R6Pen–PNA705, Pip1–PNA705 and RXR4-PNA705 (note the different concentration ranges for the three conjugates); and (c) RT-PCR analysis to measure aberrant and redirected RNA levels in HeLa pLuc705 cells. The concentration ranges are the same as for (b) above.

$1 \mu M$ in splicing redirection by RT-PCR analysis after incubation with HeLa pLuc705 cells (33). In preliminary studies we found that replacement of Trp by Leu in segment 2 resulted in a slight improvement in splicing redirection (33). When this W→L mutation was combined with replacement of segment 1 by (R-Ahx-R)$_3$ (i.e. spacing of the six Arg residues by three aminohexanoyl linkers, shown as X in Figure 1a), the activity increased further (37). Since three non-natural amino acids had been added, we shortened the peptide by deletion of RQ from segment 1 and removed the GG spacer, to give the 24-mer PNA Internalization Peptide 1 (Pip1, Figure 1a). Pip1 disulphide-conjugated to 18-mer CKPNA705K (PNA705) was tested in the HeLa cell splice redirection assay for luciferase activity (Figure 1b) and by RT-PCR analysis (Figure 1c) for amounts of aberrant and correctly spliced RNA. Pip1-PNA705 showed two to three times the fold increase in luminescence compared to R6Pen–PNA705 at similar concentrations (Figure 1b). The EC$_{50}$ in the RT-PCR assay for Pip1–PNA705 was $0.50 \pm 0.05 \mu M$,

which was about 2-fold better than R6Pen–PNA (Figure 1c) (33). RXR4–PNA705 was substantially less active in both assays with an EC$_{50}$ of splice redirection of $3–4 \mu M$ (Figure 1c). We also synthesized a conjugate of PNA705 with (R-Ahx-R)$_4$-Ahx-Cys (RXR4X), which contains an additional Ahx (X) spacer, and the EC$_{50}$ of this conjugate in splice redirection was very similar to that of RXR4-PNA705 (data not shown).

Serum stabilized Pip peptides as PNA705 conjugates

For *in vivo* studies, it is necessary to ensure that the peptide component of the conjugate is sufficiently stable to serum proteolysis so that there is a better chance of the conjugate reaching the necessary cells. We therefore developed a convenient assay based on incubation of conjugates with 20% mouse serum, observation of the loss of conjugate and determination of the fragment masses of proteolytic cleavage products by MALDI-TOF mass spectrometry. Although not fully quantitative, it is possible to identify the most vulnerable proteolysis sites very easily

from the masses of the cleavage fragments. For example, Pip1–PNA was fully cleaved within 1 h under these conditions, with the major fragment observed being consistent with cleavage between amino acids R_{17} and R_{18} (Figure 2a). Minor cleavages were observed between K_{11} and I_{12}, between K_{22} and K_{23} and between K_{23} and C_{24} (data not shown). It should be noted that no cleavage was observed within the PNA and insignificant cleavage at the disulphide linkage occurred under these conditions. Under the same serum incubation conditions, R6Pen–PNA705 was heavily degraded in the peptide component within a few minutes and cleavage was also observed between the same amino acid residues (data not shown).

A series of peptides was then synthesized iteratively aimed at altering the sequences at the identified vulnerable regions to increase their stability to serum proteolysis, but without losing significant splice redirection ability when disulphide-conjugated to PNA705. For each peptide in the series, the EC_{50} of the conjugate was measured in the RT-PCR assay and the serum stability studied by MALDI-TOF mass spectrometry (Supplementary Table 1). The culmination of this study was two candidate peptides, Pip2a ((R-Ahx-R)₃IdKILFQNdRRMKWHKB C) and Pip2b ((R-Ahx-R)₃IHILFQNdRRMKWHKBC), differing only in a single amino acid in position 11 (Supplementary Table 1). Conjugates of these peptides with PNA705 were predominantly stable for 1 h in 20% mouse serum (Figure 2b and Supplementary Table 1). RXR4–PNA705 was found also to be predominantly stable under the same serum conditions as shown in Figure 2c. In the HeLa pLuc705 cell splicing redirection assay the EC_{50} for Pip2a–PNA705 was $0.79 \pm 0.13\,\mu M$ and for Pip2b–PNA705 was $0.64 \pm 0.07\,\mu M$ (Supplementary Table 1), intermediate between that of Pip1–PNA705 and R6Pen–PNA705.

Cell uptake mechanism of Pip–PNA705 conjugates

The increased splicing redirecting activity of Pip–PNA conjugates as compared to R_6Pen–PNA705 and RXR4–PNA705 could be due to differences in their cellular uptake mechanism. Several publications have indeed pointed to non-endocytotic mechanisms or macropinocytosis as more favourable pathways. We first verified that all CPP–PNA conjugates in this series were taken up by an energy-dependent mechanism (Figure 3a). In order to delineate which endocytotic pathway was prevalent, two well-characterized inhibitors of each route were used. Chlorpromazine $(30\,\mu M)$ or K^+ depletion were used to inhibit clathrin-coated pits-mediated endocytosis. Nystatin $(50\,\mu M)$ or fillipin-III $(5\,\mu g\,ml^{-1})$ were used to inhibit caveolae-mediated endocytosis. Methyl-β-cyclo-dextrin $(2.5\,mM)$ or 5-(N-ethyl-N-isopropyl)-amiloride (EIPA) (1mM) was used to inhibit macropinocytosis. Since these inhibitors are not devoid of cytotoxicity, the concentrations and the duration of pre-incubation and of incubation were optimized to avoid any significant effect on protein synthesis (data not shown). As shown in Figure 3b for Pip2b–PNA705, chlorpromazine and K^+ depletion decreased luciferase expression by 90% and 74%, respectively, in keeping with clathrin-coated
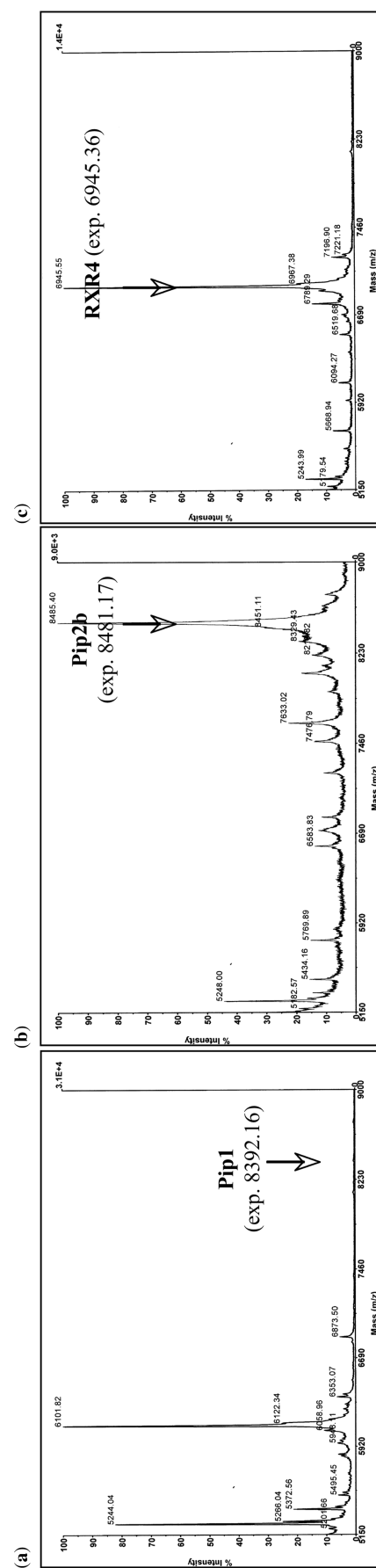

Figure 2. MALDI-TOF mass spectra of (**a**) Pip1–PNA705, (**b**) Pip2b–PNA705 and (**c**) RXR4–PNA705 after treatment for 1 h with 20% mouse serum. Expected (exp.) mass values for full-length conjugates are shown by an arrow.
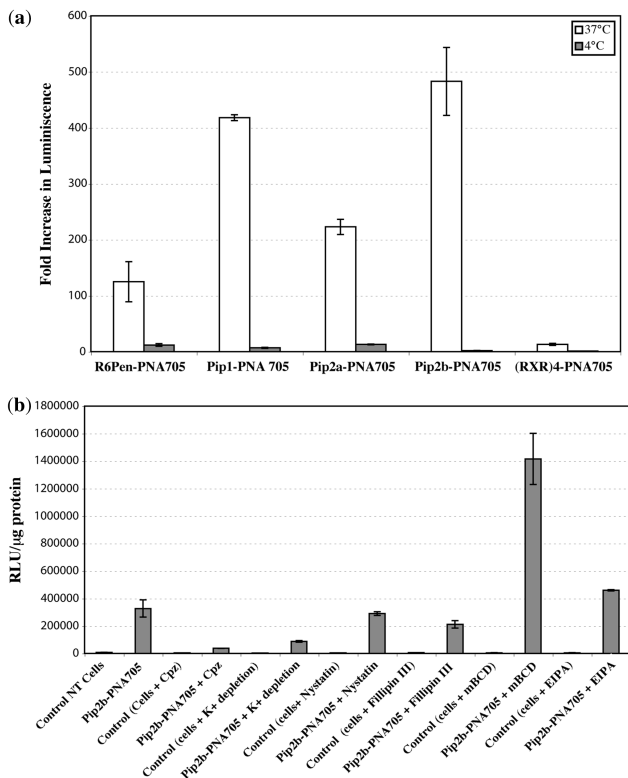
Figure 3. (a) Splicing redirection activity in HeLa pLuc705 cells treated with 1 μM R6Pen–PNA705, Pip1–PNA705, Pip2a–PNA705, Pip2b–PNA705 or RXR4–PNA705 at 37°C and 4°C suggests in each case an energy-dependent uptake mechanism. (b) The effect of endocytosis inhibitors on splicing correction activity of Pip2b–PNA705. The results are shown as relative light units per microgram protein, rather than fold-increase, because of differences in the levels of background luminescence when inhibitors are used, as seen for each control cells + inhibitor experiment. Cpz = chlorpromazine, mBCD = methyl-β-cyclodextrin, EIPA = 5-(N-ethyl-N-isopropyl)-amiloride.

pits being the major pathway of internalization. Caveolae inhibitors such as nystatin or fillipin-III had lower inhibitory effects (12% and 36%, respectively). Macropinocytosis did not seem to be involved since methyl-β-cyclodextrin increased luciferase expression while EIPA had no effect. Pip1–PNA705 and Pip2a–PNA705 showed similar results (data not shown). Pip–PNA705 conjugates thus appear to be internalized mainly through clathrin-coated pits as already proposed for Tat–PNA (38) and for RXR4–PNA or RXR4–PMO conjugates [(22) and unpublished data].

Synthesis of Pip–PNA conjugates targeted to dystrophin pre-mRNA and exon-skipping activity in cultured *mdx* muscle cells

Pip1, Pip2a, Pip2b and RXR4 peptides were each conjugated via a stable thioether linkage to a 20-mer PNA (PNADMD) that was shown previously to have activity as naked PNA in exon 23 skipping in the *mdx* mouse by direct muscle injection (14). These conjugates were incubated for 4 h with differentiated *mdx* mouse myotubes at 1 or 2 μM concentrations without any other transfection system. RNA was isolated after 20 h from the cells and

nested RT-PCR analysis was carried out to measure the levels of exon skipping (Figure 4). Pip1–PNADMD and RXR4–PNADMD each showed a small amount of exon skipping at 2 μM, but Pip2a–PNADMD and Pip2b–PNADMD showed significantly higher levels of exon skipping at both 1 and 2 μM concentrations. No exon skipping was observed for naked PNADMD. This shows that in the absence of any transfection method Pip2a and Pip2b peptide conjugation enhances substantially the cell and nuclear delivery of PNADMD into *mdx* muscle cells as compared to the other peptides. Specificity of exon skipping by PNADMD compared to a sense control PNA was observed by electroporation of 0.5 nmol quantities into the mdx myoblasts. Naked PNADMD, Pip2a–PNADMD and Pip2b–PNADMD each showed exon skipping as expected when electroporated into the cells, whereas the sense control PNA showed no exon skipping (Supplementary Figure 1).

Cell viability was checked by a standard MTS assay for Pip2a–PNADMD and Pip2b–PNADMD. No significant loss of viability was seen for *mdx* mouse muscle cells treated with 2 μM conjugate and the viability at 5 μM was ~80–85% (data not shown).

Exon skipping and dystrophin expression following intramuscular injection in the *mdx* mouse

The exon-skipping effects of naked PNADMD and PNADMD–peptide conjugates were evaluated in *mdx* mice by local intramuscular injection. Six- to eight-week-old *mdx* mice (referred to as 8 weeks) were injected with a single dose of 5 μg PNA or PNA–peptide conjugate into the TA muscle. Two weeks after injection all treated TA muscles were harvested and dystrophin-positive fibres were identified by immunohistochemistry (Figure 5a). Inspection of whole-muscle transverse sections after a single injection of PNA or PNA–peptide conjugates showed widespread and uniform distribution of dystrophin-positive fibres throughout the muscle cross-sections, except in the cases of Pip1–PNADMD-treated mice, in which only a limited number of dystrophin-positive fibres was observed, and the untreated *mdx* mouse control (Figure 5a). Of particular interest were Pip2a–PNADMD- and Pip2b–PNADMD-treated *mdx* muscles which showed a highly significant increase ($P < 0.05$) in the number of dystrophin-positive myofibres compared with those treated with PNA alone, Pip1 and RXR4–PNA conjugates compared with age-matched control *mdx* mice (Figure 5b). Consistent with these immunohistochemistry data, RT-PCR analysis showed the expected exon 23 skipped bands (Figure 5c).

DISCUSSION

Pip2a and Pip2b are representatives of a new class of cell-penetrating peptide with enhanced serum-stability and higher cell delivery potential. We chose PNA (over PMO) as the ON cargo type because of its ready synthetic accessibility and ability to be conjugated to peptides by either disulphide or stable thioether linkages. Pip2a- and Pip2b–PNA conjugates showed higher activity than
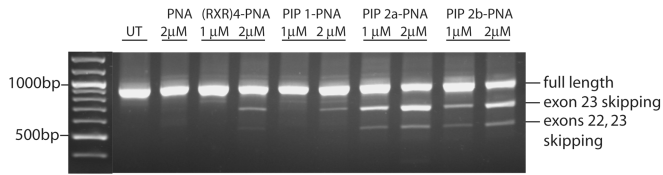
Figure 4. Exon skipping in mouse *mdx* muscle myotubes for naked PNADMD, RXR4–PNADMD, Pip1–PNADMD, Pip2a–PNADMD and Pip2b–PNADMD at 1 and 2 µM in the absence of a transfection agent.

conjugates of the well-known RXR4 peptide in redirection of splicing in HeLa cells and in exon skipping in mouse *mdx* muscle cells. The activity improvement was paralleled *in vivo* in a mouse mdx TA muscle injection model. Pip2a and Pip2b are composed of 3 peptide segments containing an Arg-rich domain, a hydrophobic segment and a broadly cationic segment. However, the structure-activity data to date from the HeLa pLuc705 experiments in this work and previous studies (33,37) point to a more subtle relationship between peptide sequence and splicing
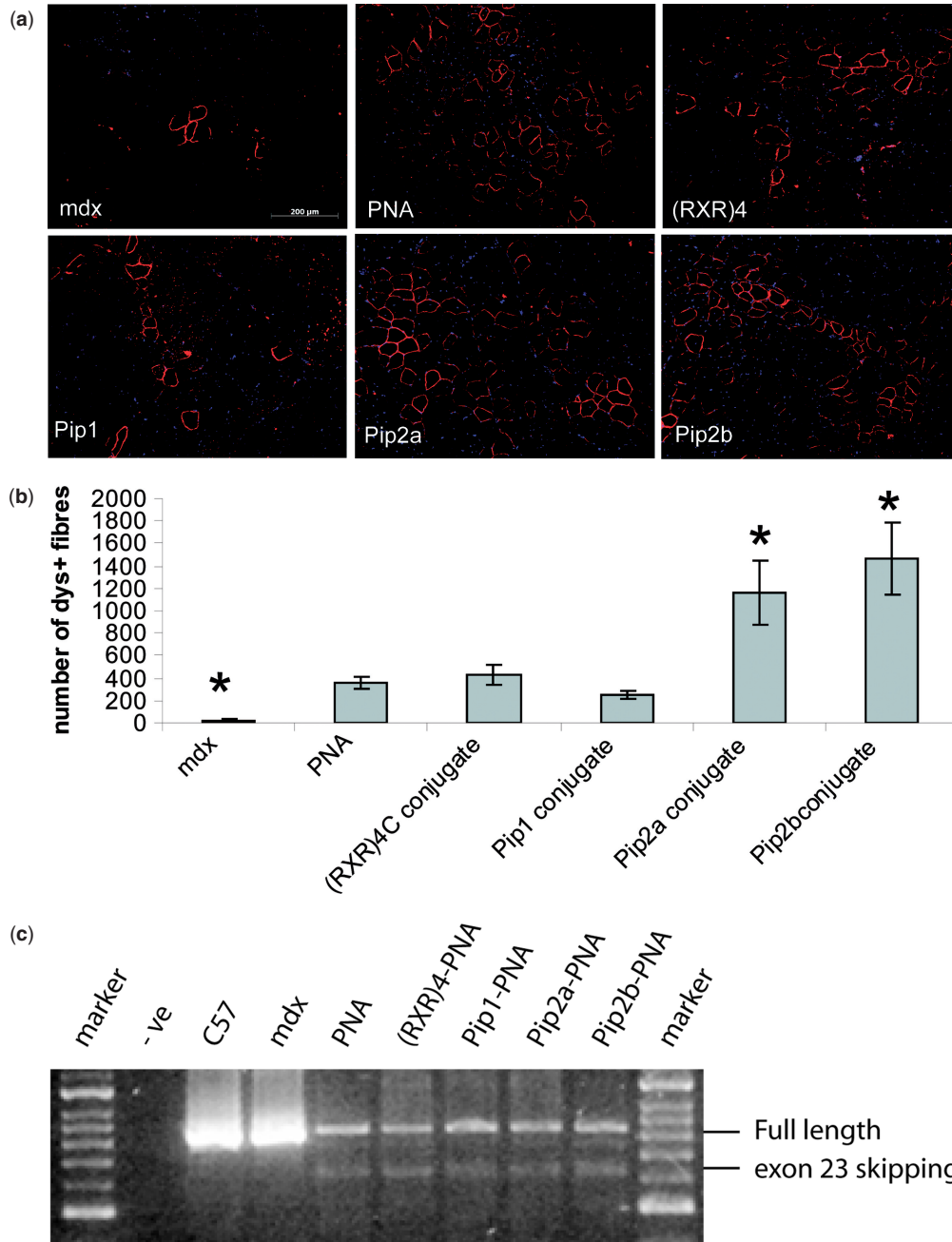

Figure 5. *In vivo* activity of Pip–PNA conjugates following intramuscular injection in *mdx* mice. Mouse i.m. injections for PNADMD and its peptide conjugates: (**a**) immunostaining of TA muscle cross-sections to detect dystrophin positive myofibres; (**b**) quantification of the number of dystrophin-positive fibres; and (**c**) RT-PCR analysis of exon skipping following intramuscular injection. C57 = control non-dystrophic mouse.

redirection than a mere juxtaposition of two cationic segments surrounding a hydrophobic segment. Within each segment there appear to be further sequence selectivities. For example, aminohexanoyl spacing within segment 1 is advantageous and some spacing of cationic residues in segment 3 also seems important (37). Note that activity levels are not related to the presence of a pH sensitive His residue in segment 3, since Lys in this position gives equal activity (Supplementary Table 1). We also reported previously that the efficiency of splicing redirection for R6Pen-PNA705 does not appear to be correlated with the membrane crossing potential of the Penetratin peptide itself (33).

Serum-stabilized Pip2a and Pip2b provided a good starting point for *in vivo* studies. These 25-mer peptides were several times more active as conjugates of PNA705 when compared to the 15-mer RXR4 peptide, which is the leading peptide used for *in vivo* studies with PMO conjugation (13,20), whilst showing similar stability to serum proteolysis under the conditions studied (Figure 2). The significantly higher activity levels observed in both muscle cell and *in vivo* assays for the longer Pip2 peptide (25-mer) compared to the shorter RXR4 (15-mer) justifies the use of a longer peptide. However, additional structure–function analysis may yet identify shorter variants with maintained or enhanced activity.

We showed recently that splicing redirection activity of a PMO705 conjugate of RXR4 (39) and a PNA705 conjugate of R6Pen (37) had much lower activities when incubated with HeLa pLuc705 cells at 4°C compared to 37°C (Figure 3a), suggesting in each case an energy-dependent cell uptake mechanism. We showed here in side-by-side comparison that both Pip2b and RXR4, when conjugated to PNA705 also appear to have energy-dependent uptake pathways, suggesting that this is a general property imparted by Arg-rich CPPs.

We and others have shown that ONs conjugated to cationic CPPs bind to heparan sulphate on the surface of HeLa cells and upon entry appear to become trapped within endocytotic vesicles (26,28,30,38). Our current study is of the effect of endocytosis inhibitors on splicing redirection (Figure 3b) and is therefore focused on the biologically active part of the conjugate that is undergoing cellular uptake. These results show clearly, and for the first time, that in HeLa pLuc705 cells clathrin-dependent endocytosis seems to be the major uptake route for biologically available Pip2b–PNA705 conjugate. The implementation of an energy-dependent endocytic pathway of cellular uptake, as opposed to direct membrane translocation, for most CPPs is still the object of debate. Most studies have relied on fluorescently labelled ONs and observation of the cellular locations by microscopy and the effect of endocytosis inhibitors on such uptake and localization (40,41), rather than a biological assay, as carried out here. Likewise, controversies still exist concerning which endocytotic pathway, macropinocytosis (40,41) or clathrin-coated pits [(38) and this study], is the major route of internalization for cationic CPPs. The cases for each of these pathways have been laid out in a recent review of cellular uptake of CPPs (42). Again we feel that monitoring a biological response in the presence of a range of

inhibitors is more relevant than relying on the uptake of fluorescent conjugates.

In preliminary studies, co-incubation of HeLa pLuc705 cells with 200 nM CPP–PNA705 conjugates and a cell-permeabilizing agent saponin led to substantial increases in luciferase production resultant from splicing redirection for both Pip2b–PNA705 and RXR4–PNA705, with the former being only marginally more active than the latter (data not shown). By contrast there is at least a 3- to 4-fold higher activity of Pip2b–PNA705 compared to RXR4–PNA705 in the absence of a transfection or permeabilization agent. This suggests that endosomal trapping is a main limitation for splicing redirection activity and that the Pip2b peptide may therefore trigger a better endosomal release than RXR4. Further experiments to confirm these observations with a range of CPP–PNAs under a variety of cell conditions are in progress and results will be reported later.

In the absence of any transfection agent, Pip2a–PNADMD and Pip2b–PNADMD showed significant exon-skipping activity in mouse *mdx* myotubes in the low micromolar range whereas RXR4–PNADMD showed only slight activity (Figure 4). Despite the quantitative differences between splicing redirection and exon skipping levels, the correlation between enhancements of activity for PNA conjugates of Pip peptides over RXR4 peptide in the HeLa cell and mouse muscle cell models is reassuring and demonstrates that better cell permeation and nuclear delivery is a general property imparted by the Pip peptide series. A similar correlation seems also to hold *in vivo*, based on immunohistological analysis of mouse TA muscles treated with Pip2a–PNADMD or Pip2b–PNADMD compared to RXR4-PNADMD (Figure 5a and b). The relatively poor activity of Pip1–PNADMD in *mdx* muscle cells and *in vivo*, in contrast to the HeLa cell result for Pip1–PNA705, presumably reflects the need for better proteolytic stability of the CPP in the *mdx* muscle system, since cell and *in vivo* data appear to correlate well.

The low levels of exon skipping at the RNA level observed for all constructs after a single local injection into the TA muscle (Figure 5c) prevented determination of differences between conjugates in exon-skipping levels. These levels are much lower than those reported in the same TA injection model for naked PMO (8), and for exon-skipping levels in systemic mouse delivery reported for naked PMO (8,43), for RXR4XB–PMO conjugate (20) or very recently for a derivative of RXR4 (B peptide, which contains two β-Ala replacements for aminohexanoyl) (44). However, in all these studies the PMO used was a 25-mer, whereas so far only a 20-mer PNA sequence has been tested here and in our previous studies in the mouse *mdx* model (14). In human myoblast cell culture, 25- to 31-mer 2′OMePS ONs were found to be significantly more effective in dystrophin exon skipping than 20-mer (45), but the effect of length of ON has not been clearly evaluated for these and other ON types *in vivo*. Note that for the first clinical trial of a PMO ON for DMD treatment a 30-mer is being used (12). We are currently investigating the optimum length for PNA *in vivo* in comparison to PMO. However for either cargo type, the

significant improvements in number of dystrophin positive fibres seen in the case of Pip2a and Pip2b suggest that these peptides are good candidates for further *in vivo* evaluation for enhancement of exon-skipping activity and may offer advantages over the RXR4 peptide series. Such *in vivo* experiments are also currently in progress.

SUPPLEMENTARY DATA

Supplementary Data are available at NAR Online.

ACKNOWLEDGEMENTS

FUNDING

REFERENCES

1. Kurreck,J. (2003) Antisense technologies. Improvement through novel chemical modifications. *Eur. J. Biochem.*, **270**, 1628–1644.
2. Lebleu,B., Moulton,H.M., Abes,R., Ivanova,G.D., Abes,S., Stein,D.A., Iversen,P.L., Arzumanov,A. and Gait,M.J. (2008) Cell penetrating peptide conjugates of steric block oligonucleotides. *Adv. Drug Deliv. Rev.*, **60**, 517–529.
3. Kole,R., Vacek,M. and Williams,T. (2004) Modification of alternative splicing by antisense therapeutics. *Oligonucleotides*, **14**, 65–74.
4. Aartsma-Rus,A. and van Ommen,G.B. (2007) Antisense-mediated exon skipping: a versatile tool with therapeutic and research applications. *RNA*, **13**, 1609–1624.
5. Dunckley,M.G., Manoharan,M., Villiet,P., Eperon,I.C. and Dickson,G. (1998) Modification of splicing in the dystrophin gene in cultured *mdx* muscle cells by antisense oligoribonucleotides. *Hum. Mol. Genet.*, **7**, 1083–1090.
6. Mann,C.J., Honeyman,K., Cheng,A.J., Ly,T., Lloyd,F., Fletcher,S., Morgan,J.E., Partridge,T.A. and Wilton,S.D. (2001) Antisense-induced exon skipping and synthesis of dystrophin in the *mdx* mouse. *Proc. Natl Acad. Sci. USA*, **98**, 42–47.
7. Lu,Q.L., Rabinowitz,A., Chen,Y.C., Yokota,T., Yin,H.F., Alter,J., Jadoon,A., Bou-Gharios,G. and Partridge,T. (2005) Systemic delivery of antisense oligoribonucleotide restores dystrophin expression in body-wide skeletal muscles. *Proc. Natl Acad. Sci. USA*, **102**, 198–203.
8. Fletcher,S., Honeyman,K., Fall,A.M., Harding,P.L., Johnsen,R.D. and Wilton,S.D. (2006) Dystrophin expression in the *mdx* mouse after localised and systemic administration of a morpholino antisense oligonucleotide. *J. Gene Med.*, **8**, 207–216.
9. Aartsma-Rus,A., Bremmer-Bout,M., Janson,A.A., den Dunnen,J.T., van Ommen,G.B. and van Deutekom,J.C. (2002) Targeted exon skipping as a potential gene correction therapy for Duchenne muscular dystropy. *Neuromusc. Disord.*, **12**, S71–S77.
10. Aartsma-Rus,A., Janson,A.A., Kaman,W.E., Bremmer-Bout,M., den Dunnen,J.T., Baas,F., van Ommen,G.B. and van Deutekom,J.C. (2003) Therapeutic antisense-induced exon skipping in cultured muscle cells from six different DMD patients. *Hum. Mol. Genet.*, **12**, 907–914.
11. van Deutekom,J.C., Janson,A.A., Ginjaar,I.B., Frankhuizen,W.S., Aartsma-Rus,A., Bremmer-Bout,M., den Dunnen,J.T., Koop,K., van der Kooi,A.J., Goemans,N.M. *et al.* (2007) Local dystrophin restoration with antisense oligonucleotide PRO051. *N. Eng. J. Med.*, **357**, 2677–2686.
12. Arechavala-Gomeza,V., Graham,I.R., Popplewell,L.J., Adams,A.M., Aartsma-Rus,A., Kinali,M., Morgan,J.E., van Deutekom,J.C., Wilton,S.D., Dickson,G. *et al.* (2007) Comparative analysis of antisense oligonucleotide sequences for targeted skipping of exon 51 during dystrophin pre-mRNA splicing in human muscle. *Hum. Gene Ther.*, **18**, 798–810.
13. Moulton,H.M. and Moulton,J.D. (2008) In Kurreck,J. (ed.), *Therapeutic Oligonucleotides.*, Royal Society of Chemistry, Cambridge, UK, pp. 43–79.
14. Yin,H., Lu,Q. and Wood,M. (2008) Effective exon skipping and restoration of dystrophin expression by peptide nucleic acid antisense oligonucleotides in *mdx* mice. *Mol. Ther.*, **16**, 38–45.
15. Gait,M.J. (2003) Peptide-mediated cellular delivery of antisense oligonucleotides and their analogues. *Cell Mol. Life Sci.*, **60**, 1–10.
16. Juliano,R.L. (2005) Peptide-oligonucleotide conjugates for the delivery of antisense and siRNA. *Curr. Opin. Mol. Ther.*, **7**, 132–138.
17. Venkatesan,N. and Kim,B.H. (2006) Peptide conjugates of oligonucleotides: synthesis and applications. *Chem. Rev.*, **106**, 3712–3761.
18. Turner,J.J., Arzumanov,A., Ivanova,G., Fabani,M. and Gait,M.J. (2006) In Langel,U. (ed.), *Cell-Penetrating Peptides*, 2nd edn. CRC Press, Boca Raton, pp. 313–328.
19. Fabani,M.M., Ivanova,G.D. and Gait,M.J. (2008) In Kurreck,J. (ed.), *Therapeutic Oligonucleotides*. Royal Society of Chemistry, Cambridge, UK, pp. 80–102.
20. Fletcher,S., Honeyman,K., Fall,A.M., Harding,P.L., Johnsen,R.D., Steinhaus,J.P., Moulton,H.M., Iversen,P.L. and Wilton,S.D. (2007) Morpholino oligomer-mediated exon skipping averts the onset of dystrophic pathology in the *mdx* mouse. *Mol. Ther.*, **151**, 587–592.
21. Kang,S.-H., Cho,M.-J. and Kole,R. (1998) Up-regulation of luciferase gene expression with antisense oligonucleotides: implications and applications in functional assay development. *Biochemistry*, **37**, 6235–6239.
22. Abes,S., Moulton,H.M., Clair,P., Prevot,P., Youngblood,D.S., Wu,R.P., Iversen,P.L. and Lebleu,B. (2006) Vectorization of morpholino oligomers by the (R-Ahx-R)₄ peptide allows efficient splicing correction in the absence of endosomolytic agents. *J. Control. Release*, **116**, 304–313.
23. Abes,S., Moulton,H.M., Turner,J.J., Clair,P., Richard,J.-P., Iversen,P.L., Gait,M.J. and Lebleu,B. (2007) Peptide-based delivery of nucleic acids: design, mechanism of uptake and applications to splice-correcting oligonucleotides. *Biochem. Soc. Trans.*, **35**, 53–55.
24. Bendifallah,N., Rasmussen,F.W., Zachar,V., Ebbesen,P., Nielsen,P.E. and Koppelhus,U. (2006) Evaluation of cell-penetrating peptides (CPPs) as vehicles for intracellular delivery of antisense peptide nucleic acid (PNA). *Bioconjugate Chem.*, **17**, 750–758.
25. El-Andaloussi,S., Johansson,H.J., Lundberg,P. and Langel,U. (2006) Induction of splice correction by cell-penetrating peptide nucleic acids. *J. Gene Med.*, **8**, 1262–1273.
26. Abes,S., Williams,D., Prevot,P., Thierry,A.R., Gait,M.J. and Lebleu,B. (2006) Endosome trapping limits the efficiency of splicing correction by PNA-oligolysine conjugates. *J. Control. Release*, **110**, 595–604.
27. Richard,J.-P., Melikov,K., Vivès,E., Ramos,C., Verbeure,B., Gait,M.J., Chernomordik,L.V. and Lebleu,B. (2003) Cell-penetrating peptides. A re-evaluation of the mechanism of cellular uptake. *J. Biol. Chem.*, **278**, 585–590.
28. Turner,J.J., Ivanova,G.D., Verbeure,B., Williams,D., Arzumanov,A., Abes,S., Lebleu,B. and Gait,M.J. (2005) Cell-penetrating peptide conjugates of peptide nucleic acids (PNA) as inhibitors of HIV-1 Tat-dependent trans-activation in cells. *Nucleic Acids Res.*, **33**, 6837–6849.
29. Wolf,Y., Pritz,S., Abes,S., Bienert,M., Lebleu,B. and Oehlke,J. (2006) Structural requirements for cellular uptake and antisense activity of peptide nucleic acids conjuagted with various peptides. *Biochemistry*, **45**, 14944–14954.
30. Koppelhus,U., Awasthi,S.K., Zachar,V., Holst,H.U., Ebbeson,P. and Nielsen,P.E. (2002) Cell-dependent differential cellular uptake

of PNA, peptides and PNA-peptide conjugates. *Antisense Nucleic Acid Drug Dev.*, **12**, 51–63.

31. Kaihatsu,K., Huffman,K.E. and Corey,D.R. (2004) Intracellular uptake and inhibition of gene expression by PNAs and PNA-peptide conjugates. *Biochemistry*, **43**, 14340–14347.

32. Shiraishi,T., Pankratova,S. and Nielsen,P.E. (2005) Calcium ions effectively enhance the effect of antisense peptide nucleic acids conjugated to cationic Tat and oligoarginine peptides. *Chem. Biol.*, **12**, 923–929.

33. Abes,S., Turner,J.J., Ivanova,G.D., Owen,D., Williams,D., Arzumanov,A., Clair,P., Gait,M.J. and Lebleu,B. (2007) Efficient splicing correction by PNA conjugation to an R₆-Penetratin delivery peptide. *Nucleic Acids Res.*, **35**, 4495–4502.

34. Turner,J.J., Williams,D., Owen,D. and Gait,M.J. (2005) Disulfide conjugation of peptides to oligonucleotides and their analogues. *Curr. Protoc. Nucleic Acid Chem.*, 4.28.1–4.28.21.

35. Roberts,K.D., Lambert,J.N., Ede,N.J. and Bray,A.M. (1998) Efficient synthesis of thioether-based cyclic peptide libraries. *Tetrahedron Lett.*, 8357–8360

36. Turner,J.J., Arzumanov,A.A. and Gait,M.J. (2005) Synthesis, cellular uptake and HIV-1 Tat-dependent trans-activation inhibition activity of oligonucleotide analogues disulphide-conjugated to cell-penetrating peptides. *Nucleic Acids Res.*, **33**, 27–42.

37. Ivanova,G.D., Arzumanov,A.A., Turner,J.J., Fabani,M.M., Abes,R., Lebleu,B. and Gait,M.J. (2008) RNA targeting in cells by peptide conjugates of peptide nucleic acids (PNA). *Collect. Symp. Ser.*, **10**, 103–111.

38. Richard,J.P., Melikov,K., Brooks,H., Prevot,P., Lebleu,B. and Chernomordik,L.V. (2005) Cellular uptake of unconjugated TAT peptide involves clathrin-dependent endocytosis and heparan sulfate receptors. *J. Biol. Chem.*, **280**, 15300–15306.

39. Abes,R., Arzumanov,A., Moulton,H.M., Abes,S., Ivanova,G.D., Iversen,P.L., Gait,M.J. and Lebleu,B. (2007) Cell-penetrating-peptide-based delivery of oligonucleotides: an overview. *Biochem. Soc. Trans.*, **35**, 775–779.

40. Nakase,I., Niwa,M., Takeuchi,T., Sonomura,K., Kawabata,N., Koike,Y., Takehashi,M., Tanaka,S., Ueda,K., Simpson,J.C. *et al.* (2004) Cellular uptake of arginine-rch peptides: roles for macropinocytosis and actin rearrangement. *Mol. Ther.*, **10**, 1011–1022.

41. Kaplan,I.M., Wadia,J.S. and Dowdy,S.F. (2005) Cationic TAT peptide transduction domain enters cells by macropinocytosis. *J. Control. Release*, **102**, 247–253.

42. Patel,L.N., Zaro,J.L. and Shen,W.-C. (2007) Cell penetrating peptides: intracellular pathways and pharmaceutical perspectives. *Pharm. Res.*, **24**, 1977–1992.

43. Alter,J., Lou,F., Rabinowitz,A., Yin,H., Rosenfeld,J., Wilton,S.D., Partridge,T.A. and Lu,Q.L. (2006) Systemic delivery of morpholino oligonucleotide restores dystrophin expression bodywide and improves dystrophic pathology. *Nat. Med.*, **12**, 175–177.

44. Jearawiriyapaisarn,N., Moulton,H.M., Buckley,B., Roberts,J., Sazani,P., Fucharoen,S., Iversen,P.L. and Kole,R. (2008) Sustained dystrophin expression induced by peptide-conjugated morpholino oligomers in the muscles of *mdx* mice. *Mol. Ther.*, **16**, 1624–1629.

45. Harding,P.L., Fall,A.M., Honeyman,K., Fletcher,S. and Wilton,S.D. (2007) The influence of antisense oligonucleotide length on dystrophin exon skipping. *Mol. Ther.*, **15**, 157–166.